2D EXTENSION OF GEM (THE GENERALIZED ECR ION SOURCE MODELING CODE）*

L. Zhao#, J. S. Kim, B. Cluggish,
FAR-TECH, Inc., San Diego, CA 92121, U.S.A.

Abstract

To model electron cyclotron resonance (ECR) ion sources, GEM [1] is being extended to two dimensions (2D) by adding a radial dimension. The electron distribution function (EDF) is calculated on each magnetic flux surface using a bounce-averaged Fokker-Planck code with a 2D ECR heating (ECRH) model. The ion fluid model is also being extended to 2D by adding collisional radial transport terms. All species in ECRIS are balanced by assuming quasi-neutrality in each cell and the plasma potential is calculated by maintaining the ambipolarity globally. The graphical user interface (GUI) and parallel computing ability of GEM make it an easy-to-use tool for ECRIS research. Numerical results and comparisons with experimental data are presented here.

INTRODUCTION

Extensive experimental results on ECR ion sources (ECRIS) have been obtained in recent years. Many theoretical and numerical studies based on these experimental results are published. Usually, ECRIS plasma parameters, such as density and temperature, are the input variables in many numerical models [2], but these methods are limited by the lack of detailed diagnostics on ECRIS devices. FAR-TECH, Inc. has developed a toolset, GEM, to simulate ECRIS plasma using only experimental knobs, such as device geometry, field profile, gas pressure, rf power, etc. as input. GEM 1D self-consistently calculates axial steady-state plasma profiles and charge state distributions (CSD) of the output beam by solving for the EDF using bounce-averaged Fokker Planck equation and highly collisional ions using 1D fluid model. GEM 1D has obtained some numerical results consistent with experiments [1]. However, the further applications of GEM to beam capture [3] and beam extraction simulation require GEM to be extended to 2D to acquire both axial and radial profiles of the plasma parameters. This paper presents the modeling theories that are implemented in GEM 2D and the results from preliminary GEM 2D runs.

MAGNETIC FIELD CONFIGURATION

As an example application, we have used GEM to model the ECR plasma in ECR-I device [4] at Argonne National Laboratory. It is a typical ECRIS device with minimum-B configuration. In GEM, the magnetic field is fitted to the experimental measurements and averaged over the azimuthal angle. The radial grids are the magnetic flux surfaces for GEM 2D calculations since the electrons are collisionless and only move on the flux surfaces. The details of the device configuration and magnetic field are discussed in the following paragraphs.

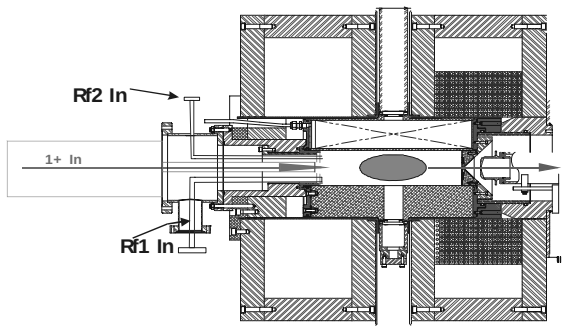

Figure 1: ANL ECR-I device which is used as a charge breeder. The coils and the multicusp magnets provide min-B configuration for the plasma confinement.

The ECR-I device

A sketch of the device is shown in Fig. 1. The plasma column is generated by electron cyclotron resonance heating and confined in the centre of the device by a magnetic field generated by the coils at two ends and the multicusps. It works as a charge-breeder if a beam of +1 ions are injected from the injection end (left end in Fig. 1). The ions with high charge states are collected at the extraction end (right end in Fig.1) as the output of ECRIS. The basic parameters in our simulation are:

- Device length=0.29 m, diameter=0.08 m.
- rf frequency=10 GHz, rf forward power =323 W, reflected power =70 W.
- Gas Oxygen ~ 1.2e-7 Torr, Argon ~ 1.0e-16 Torr.
- Mirror ratio~4.5 at injection and 3 at extraction.

Magnetic field

The magnetic field on ECR-I is a typical minimum-B structure which is composed by a mirror field and a hexapole field. The mirror field is generated by coils at two ends of the vessel. The hexaplole field is generated by multicusp shown in Fig.1. In GEM 2D, the mirror field is fitted to the experimental data with imaginary current rings, the cusp field is fitted to the experimental data using following approximate hexapole field formula:

$$B(r) = B_a \left(\frac{r}{r_a} \right)^2 \cos 3\theta, \qquad (1)$$

where θ is the azimuthal angle, B_a =0.8T, r_a =0.04m. As is shown in the contour plots (Fig. 2) of the magnetic field, the magnetic field and the ECR resonance surfaces

*Work supported by UD DOE SBIR DE-FG02-04ER83954
#zhao@far-tech.com

actually depend on z, r, θ. In GEM 2D, the magnetic field is azimuthally averaged to eliminate θ dependence.

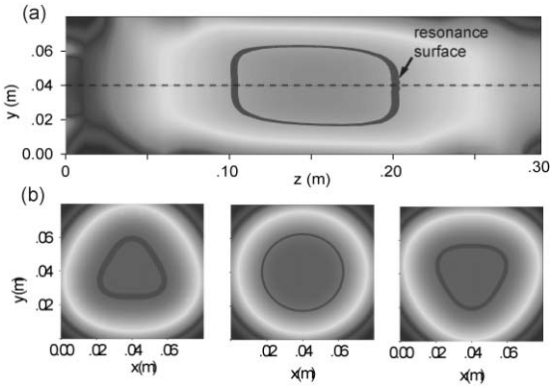

Figure 2: Contour plots of the minimum-B field configuration on an ECRIS. a) Field contour at y-z plane. b) Field contours at x-y plane at, from left to right, z~0.1, 0.15 and 0.2 m. The closed curve in the figure is the projection of rf resonance surface.

The mirror-like, azimuthally averaged 2D magnetic field profile and magnetic field flux surfaces are plotted in Fig. 3. The radial grids are the flux surfaces that are evenly distributed on the midplane (Fig. 3a) and then extended to the whole chamber along the field lines. The field strength along the field lines are plotted in Fig. 3b.

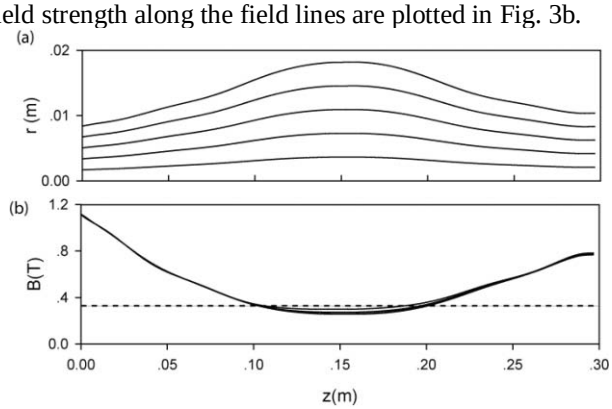

Figure 3: a) Radial grids are tied onto the magnetic field lines, in this case, number of radial grids=6. b) Magnetic field strength along the field lines in a). The dashed line is the resonance field, B_{res}=0.357 T.

PHYSICAL MODELS OF GEM 2D

Fokker-Planck Electron modeling

In general ECR plasma, electrons are hot (temperature >1 keV) and collisionless, i.e., the electron collision frequency is much less than the bouncing frequency, and the EDF is non-Maxwellian. A 0D bounce-averaged Fokker-Planck code [5] is feasible for predicting EDF on the midplane. The Fokker-Planck equation on midplane:

$$\frac{\partial f_e}{\partial t} + \vec{v} \bullet \frac{\partial f_e}{\partial \vec{x}} + \frac{\vec{F}}{m_e} \bullet \frac{\partial f_e}{\partial \vec{v}} = \left(\frac{\partial f_e}{\partial t}\right)_{coll} + C_{FP}^{S}(v,\theta) + C_{FP}^{rf}(v,\theta) \quad (2)$$

The collision term $\left(\frac{\partial f_e}{\partial t}\right)_{coll}$ and the source term $C_{FP}^{S}(v,\theta)$ in Eq. 2 are calculated by bounce-averaging method, i.e., the plasma parameters are averaged over the bouncing orbit in the mirror field by assuming that the bouncing frequency is much greater than the collision frequency. The EDF is mapped axially along the magnetic flux surface through electron energy conservation and magnetic momentum conservation. Since the radial transport of electrons is ineligible, EDF on each radial grid can be calculated independently..

The ECR heating term $C_{FP}^{rf}(v,\theta)$ in Eq. 2 is a quasi-linear term to implement ECR heating which can also be calculated by a bounce-averaging method. The rf power deposited in the plasma is distributed only near the resonance surface.

Neutral modeling

Since neutrals are not constrained by magnetic field geometry, an ideal neutral modeling should be a complete 3D model with actual background plasma profiles as input. However, our 2D model does not provide the exact plasma spatial profiles during the process of relaxing to the steady-state. We use a simple 1D radial averaged model to predict the neutral distribution in the plasma. The change of the neutrals in the plasma is balanced by the neutrals outside of the plasma and the neighbouring cells. The neutral distribution is averaged over radial direction and the neutral temperature is room temperature everywhere as the neutral mean-free path is much longer than the device.

2D fluid ion modeling

Ions in ECR plasma are highly collisional because the typical ion temperature is only ~1eV. For this reason, ions can be treated by a fluid model. The 2D ion continuity equation for ions of species *j* and charge state *q* is

$$\frac{\partial n_{j,q}}{\partial t} + \frac{1}{A_z}\frac{\partial}{\partial z}\left[A_z n_{j,q} u_z\right] + \frac{1}{r}\frac{\partial}{\partial r}\left[r n_{j,q} u_{r\,j,q}\right] = S_{j,q}, \quad (3)$$

where A_z is the cross-section of the grid *z*, u_z and u_r are ion velocity in axial and radial direction, *S* is the source of the ion including ions gained or lost due to ionization and charge-exchange. The axial velocity u_z is the same for different ion species since the motion of the ions are strongly coupled in axial direction, but the radial velocity u_r could be different if ion-ion Coulomb collision rate is less than ion cyclotron frequency. u_r can be calculated by solving the radial and azimuthal momentum equations:

$$m_j n_{j,q} \frac{\partial u_{j,qr}}{\partial t} = q n_{j,q} e(E_r + u_{j,q\theta} B) - k_B T_{j,q} \frac{\partial n_{j,q}}{\partial r} - F_r^{jk}$$
$$F_r^{jk} = n_{j,q} \sum_{k,p} \mu_{jk} n_{k,p} K_{j,q\to k,p} (u_{j,qr} - u_{k,pr}) \quad (4)$$
$$m_j n_{j,q} \frac{\partial u_{j,q\theta}}{\partial t} = -q n_{j,q} e v_{j,qr} B - F_\theta^{jk}$$
$$F_\theta^{jk} = n_{j,q} \sum_{k,p} \mu_{jk} n_{k,p} K_{j,q\to k,p} (u_{j,q\theta} - u_{k,p\theta})$$

E and B are the electric and magnetic fields in the plasma and F is the friction force due to ion-ion Coulomb collisions. The convection term can be ignored since the changing of the velocities is slow when plasma is approaching steady-state.

The axial ion momentum equation is

$$\frac{\partial u_{j,q}}{\partial t} = -u_{j,qr} \frac{\partial u_z}{\partial r} - u_{j,q} \frac{\partial u_z}{\partial z} - \frac{k_B T_{j,q}}{m_j} \frac{1}{n_{j,q}} \frac{\partial n_{j,q}}{\partial z} \quad (5)$$
$$+ \frac{1}{n_{j,q}} S_{j,q}^{in} \left(\langle u \rangle^{in} - u_z \right) + \frac{qe}{m_j} E_z$$

The axial electrical field can be solved from this equation together with electron continuity equation and ambipolar assumption.

RESULTS

We did a non-coupling GEM 2D test to verify the consistency of the code with GEM 1D. The radial transport of the ions is turned off by setting all radial terms in fluid model as zero. The non-coupling GEM 2D run is performed on 6 radial grids. The magnetic field and rf heating profile are forced to be identical for each radial grids. The results are consistent with GEM 1D, as shown in Fig. 4.

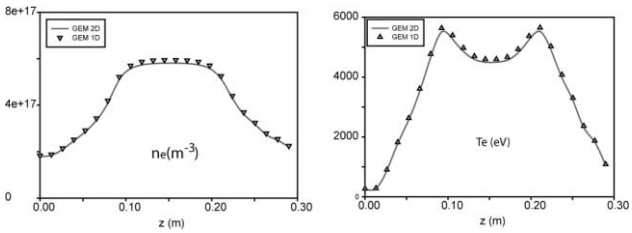

Figure 4: Plasma density and temperature profiles calculated by non-coupling GEM 2D and the comparisons with GEM 1D result.

The results of a preliminary GEM 2D run are obtained by setting the number of radial grids=6, the plasma radius=2 cm, within ECR heating zone. The radial transport of the ions is turned on. The plasma heating profile is shown in Fig 5. Rf power is deposited around the ECR surface with more power going into the center of the plasma.

The surface plots of steady-state electron density and temperature are shown in Fig. 6. Plasma density is peaked at the midplane then drops near the plasma edge due to radial transport. The temperature profile is pretty flat across the radial coordinates. The two peaks on the temperature profile along z-axis are the positions of ECR heating.

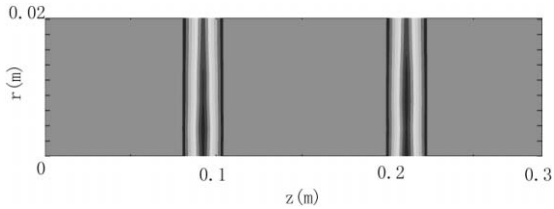

Figure 5: The profile of rf power density that is deposited in the plasma.

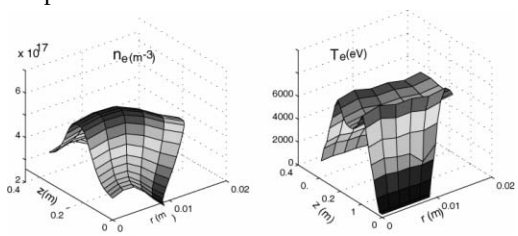

Figure 6: GEM 2D results: profiles of the plasma density and temperature.

CONCLUSIONS

GEM 1D is successfully extended to 2D by adding a radial dimension to the plasma parameters. The collisionless, non-Maxwellian electrons are modelled independently on each radial grid by solving the Fokker-Planck equation using a bounce-averaging method. The neutral profile is averaged in radial direction, i.e., it has only axial dependence. The neutral temperature is assumed to be room temperature everywhere. The 1D ion fluid equations are extended to 2D by adding radial transport terms caused by ion-ion Coulomb collisions. The non-coupling GEM 2D run, by turning of the ion radial transport, has obtained consistent results with GEM 1D. When the 2D ion fluid model is switched on, the coupling GEM 2D run gives similar results as GEM 1D except that plasma profiles are in 2D.

Future improvements of GEM 2D will be focused on the detailed calculation methods, such as the gradient calculations in the 2D fluid model, the convergence study and extending the simulation to cold plasma region.

REFERENCES

[1] D.H. Edgell, J.S. Kim, and I.N. Bogatu, R.C. Pardo and R.C. Vondrasek, *Rev. Sci. Instrum.*, **73**, 641 (2002).

[2] M. Cavenago, O. Kester, T.Lamy and P. Sortais, R*ev. Sci. Instrum.* **73**, 537 (2002)

[3] J.S. Kim, C. Liu, D.H. Edgell, and R. Pardo, *Rev. Sci. Instrum.*, **77**, 03B106 (2006).

[4] F. Ames, R. Baartman, P. Bricault, K. Jayamanna, M. McDonald, M. Olivo, P. Schmor, D.H.L. Yuan, and T. Lamy, *Rev. Sci. Instrum.*, **77**, 3B103 (2006).

[5] A. Mirin, M. McCoy, G. Tomaschke and J. Killeen, *Comput. Phys. Commun.* **81**, 403 (1994)

